Langmuir
Article
pubs.acs.org/Langmuir

A Versatile Approach to Fabricate Ordered Heterogeneous Bull's-Eye-Like Microstructure Arrays

Difu Zhu, Xiao Li, Gang Zhang, Wei Li,† Xun Zhang, Xuemin Zhang, Tieqiang Wang, and Bai Yang*

State Key Laboratory for Supramolecular Structure and Materials, College of Chemistry, Jilin University, Changchun 130012, P. R. China. † Current address: Max Planck Institute of Colloids and Interfaces, D-14424, Potsdam, Germany.

Received September 28, 2009. Revised Manuscript Received October 23, 2009

In this paper, ordered heterogeneous bull's-eye-like microstructure arrays were fabricated through a simple two-step method on gold substrate with patterned self-assemble monolayers (SAMs). First, we prepared ordered polymer dot arrays on the SAMs patterned gold substrate by SAMs-direct dewetting. Subsequently, by manipulating concentration-controlled dewetting process, ordered ring arrays were obtained on the dot arrays patterned surface under the protection of water droplets. Namely, ordered bull's-eye-like structure arrays were fabricated successfully. The mechanism of these two kinds of dewetting process has been investigated in detail. And due to these two steps were independent, different materials could be simply introduced to the current system. Therefore, ordered homogeneous and heterogeneous bull's-eye-like structure arrays such as poly(*N*-vinylcarbazole) (PVK) (dot)/PVK (ring), PVK/5,12-ditetradecylquinolino[2,3-*b*]-acridine-7,14(5*H*,12*H*)-dione (DTQA), and PVK/Fe_3O_4 nanoparticles were obtained. This straightforward method may open up new possibilities for practical use of microchips with binary heterogeneous structure arrays.

Introduction

In modern science and technology, patterning technologies have been extensively applied in various fields[1,2] such as the fabrication of optical devices,[3,4] biochips,[5,6] electronic devices,[7] sensors,[8,9] actuators,[10] and microelectronic circuits.[11] The drawbacks of conventional photolithography technique involve high cost and limited direct applicability to most materials. Consequently, soft lithography,[12] embossing,[13] cold-welding,[14] selective deposition,[15−17] and other alternative patterning techniques[18,19] have been developed. In the past decade, techniques based on dewetting[20−23] and condensation on physicochemically heterogeneous substrates appeared as simple methods to engineer ordered mesoscale structures in soft materials without use of lithographic processes. For example, the "breath figures" technique has attracted much interest in the past few years since it provide a simple and low cost templating method that is capable of producing patterns with periodicity within a size range from 50 nm to 20 mm.[24,25] By this technique, long-range ordered ring arrays can be obtained using a water droplet template on a substrate patterned with self-assembled monolayers (SAMs).[26−29] Despite the techniques mentioned above are simple and costless, they tend to form single-component patterns.

Heterogeneous patterned surface exhibits a fascinating breadth of properties for applications in a range of fields, such as microelectromechanics,[30] optoelectronics,[31] microwave devices,[32] data storage,[33] photocatalysis surface,[34] and surface-enhanced Raman scattering (SERS),[35] which based on the interaction between different phases when stimulated by external fields. Compared with the traditional patterning technique, some non-traditional approaches including polymer phase separation,[36]

*Corresponding author. E-mail: byangchem@jlu.edu.cn.

(1) Geissler, M.; Xia, Y. N. *Adv. Mater.* **2004**, *16*, 1249.
(2) Woodson, M.; Liu, J. *Phys. Chem. Chem. Phys.* **2007**, *9*, 207.
(3) Mele, E.; Benedetto, F. D.; Persano, L.; Cingolani, R.; Pisignano, D. *Nano Lett.* **2005**, *5*, 1915.
(4) Park, H.; Cheng, X. *Nanotechnology* **2009**, *20*, 245308.
(5) Szili, E.; Thissen, H.; Hayes, J. P.; Voelcker, N. *Biosens. Bioelectron.* **2004**, *19*, 1395.
(6) Kurkuri, M. D.; Driever, C.; Johnson, G.; McFarland, G.; Thissen, H.; Voelcker, N. H. *Biomacromolecules* **2009**, *10*, 1163.
(7) Baba, A.; Knoll, W. *Adv. Mater.* **2003**, *15*, 1015.
(8) Hagleitner, C.; Hierlemann, A.; Lange, D.; Kummer, A.; Keness, N.; Brand, O.; Baltes, H. *Nature* **2001**, *414*, 293.
(9) Adhikari, B.; Majumdar, S. *Prog. Polym. Sci.* **2004**, *29*, 699.
(10) Takashima, W.; Kanamori, K.; Pandey, S. S.; Kaneto, K. *Sens. Actuators B* **2005**, *110*, 120.
(11) Sirringhaus, H.; Kawase, T.; Friend, R. H.; Shimoda, T.; Inbasekaran, M.; Wu, W.; Woo, E. P. *Science* **2000**, *290*, 2123.
(12) Xia, Y. N.; Whitesides, G. M. *Annu. Rev. Mater. Sci.* **1998**, *28*, 153.
(13) Chou, S. Y.; Krauss, P. R.; Renstrom, P. J. *Science* **1996**, *272*, 85.
(14) Kim, C.; Burrows, P. E.; Forrest, S. R. *Science* **2000**, *288*, 831.
(15) Huang, Z.; Wang, P.; MacDiarmid, A. G.; Xia, Y. N.; Whitesides, G. M. *Langmuir* **1997**, *13*, 6480.
(16) Qin, D.; Xia, Y. N.; Xu, B.; Yang, H.; Zhu, C.; Whitesides, G. M. *Adv. Mater.* **1999**, *11*, 1433.
(17) Park, M. H.; Jang, Y. J.; Sung-Suh, H. M.; Sung, M. M. *Langmuir* **2004**, *20*, 2257.
(18) Luo, C. X.; Xing, R. B.; Han, Y. C. *Surf. Sci.* **2004**, *552*, 139.
(19) Gleiche, M.; Chi, L. F.; Fuchs, H. *Nature* **2000**, *403*, 173.
(20) Braun, H. G.; Meyer, E. *Thin Solid Films* **1999**, *345*, 222.
(21) Higgins, A. M.; Jones, R. A. L. *Nature* **2000**, *404*, 476.
(22) Khanal, B. P.; Zubarev, E. R. *Angew. Chem., Int. Ed.* **2007**, *46*, 2195.
(23) Kargupta, K.; Sharma, A. *Langmuir* **2003**, *19*, 5153.
(24) Bunz, U. H. F. *Adv. Mater.* **2006**, *18*, 973.
(25) Gómez-Segura, J.; Kazakova, O.; Davies, J.; Josephs-Franks, P.; Vecianaa, J.; Ruiz-Molina, D. *Chem. Commun.* **2005**, *45*, 5615.
(26) Meyer, E.; Braun, H. G. *Macromol. Mater. Eng.* **2000**, *276*/*277*, 44.
(27) Lu, G.; Li, W.; Yao, J.; Zhang, G.; Yang, B.; Shen, J. *Adv. Mater.* **2002**, *14*, 1049.
(28) Zhang, L.; Si, H. Y.; Zhang, H. L. *J. Mater. Chem.* **2008**, *18*, 2660.
(29) Poyato, R.; Calzada, M. L.; Pardo, L. *J. Appl. Phys.* **2005**, *97*, 034108.
(30) Nakamura, A.; Ishihara, J.; Shigemori, S.; Yamamoto, K.; Aoiki, T.; Gotoh, H.; Temmyo, J. *J. Appl. Phys.* **2005**, *44*, L4.
(31) Kalinin, S. V.; Bonnell, D. A.; Alvarez, T.; Lei, X. J.; Hu, Z. H.; Shao, R.; Ferris, J. H. *Adv. Mater.* **2004**, *16*, 795.
(32) Majumder, S. B.; Jain, M.; Martinez, A.; Katiyar, R. S.; Van Keuls, F. W.; Miranda, F. A. *J. Appl. Phys.* **2001**, *90*, 896.
(33) Ahn, C. H.; Rabe, K. M.; Triscone, J. M. *Science* **2004**, *303*, 488.
(34) Wu, Y.; Yan, H.; Yang, P. *Top. Catal.* **2002**, *19*, 197.
(35) Ruan, W. D.; Wang, C. X.; Ji, N.; Lu, Z. C.; Zhou, T. L.; Zhao, B.; Lombard, J. R. *Langmuir* **2008**, *24*, 8417.
(36) Park, M.; Harrison, C.; Chaikin, P. M.; Register, R. A.; Adamson, D. H. *Science* **1997**, *276*, 1401.

electron-beam lithography (EBL),[37] templated growth,[38] interference lithography,[39] nanotransfer printing,[40] and robotic deposition[41] have been developed in fabrication of heterogeneous pattern. Although various methods above are well-established, they suffered from drawbacks such as rigorous experimental conditions, time/cost wasting, or less universal. Furthermore, the key bottleneck of the formation of ordered heterogeneous structure is the stringent requirement on feature realignment between the multiple patterning steps which are required in order to form heterogeneous patterns composed of more than two materials. Accordingly, fabricating the ordered heterogeneous patterned surface through a simply approach remains a fundamental challenge. Herein, we report a simple and versatile method to fabricate a multifunctional surface with ordered heterogeneous bull's-eye-like structure arrays.

We demonstrated a convenient method to fabricate ordered two-dimension (2D) polymer ring arrays on SAMs-patterned surfaces by modified "breath figures" technique.[27] From experimental process, we found that water droplets play an important role in the whole operation, since that they serve as not only a template in the formation of ring arrays but also a "shield" on the hydrophilic SAM. Therefore, in this paper, the entire experiment was divided into two processes by the water droplets: one is the SAMs-direct dewetting process (formation of dot arrays); the other is the water-droplets-directed and concentration-controlled dewetting process (formation of ring arrays). Through two independent processes, ordered bull's-eye-like structure (a ring with a dot in the middle) arrays have been fabricated on the gold substrate. As a result of the universality of this method, ordered large-area homogeneous and heterogeneous bull's-eye-like structure arrays have been obtained, such as poly(*N*-vinylcarbazole) (PVK) (dot)/PVK (ring), PVK/5,12-ditetradecylquinolino [2,3-*b*]acridine-7,14(5*H*,12*H*)-dione (DTQA), and PVK/Fe_3O_4 nanoparticals. Accordingly, this simple method could be used for microchips with binary heterogeneous structure arrays. The novel ordered bull's-eye arrays also could subsequently be used as resist for reactive ion etching to fabricate the unprecedented field emission devices (FEDs).

Experimental Section

Materials. Thin films of gold were prepared using thermal evaporation onto glass cover slides with surfaces that had been primed with a thin layer of chromium, which were cleaned by immersion in piranha solution (7:3 concentrated H_2SO_4/30% H_2O_2) for 20 min, and then rinsed repeatedly with Milli-Q water (18.2 MΩ cm^{-1}) and absolute ethanol. The substrates were dried in a nitrogen stream before used. 16-Mercaptohexadecanoic acid (MHA), hexadecanethiol (HDT), polystyrene (PS, M_w = 3600) and poly(*N*-vinylcarbazole) (PVK, M_w = 90000) were purchased from Aldrich. Poly(dimethylsiloxane) (PDMS) elastomer kits (Sylgard 184) were purchased from Dow Corning (Midland, MI). Chloroform, sulfuric acid, and hydrogen peroxide were analytical grade and used as received. The light-emitting small molecular-based organic complexes including 5,12-ditetradecylquinolino[2,3-*b*]acridine-7,14(5*H*,12*H*)-dione (DTQA), 4-(dicyanomethylene)-2-*tert*-butyl-6-(1,1,7,7-tetramethyljulolidin-4-yl-vinyl)-4*H*-pyan (DCJTB) and (E)-9,9′-(4,4′-(but-1-en-3-yne-1,4-diyl)bis(4,1-phenylene))bis(9*H*-carbazole) (CPEY) were purchased from Jilin OLED Material Technology Company, Ltd. (Changchun, China), and schematics of the molecular structure are shown in the Supporting Information. Oleic-acid-stabilized Fe_3O_4 magnetite nanoparticles were synthesized according to the literature.[42]

Scheme 1. The Process of Ordered Bull's-Eye-Like Structure Arrays Formation[a]

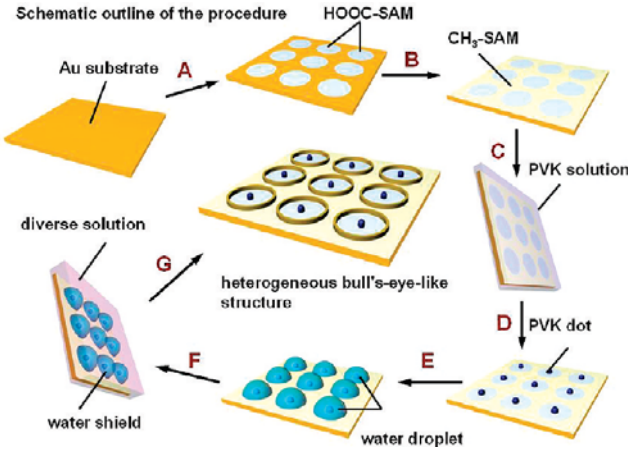

[a] Key: A, microcontact printing (μCP) with $HOOC(CH_2)_{15}SH$; B, washing with CH_3-$(CH_2)_{15}SH$ solution; C, washing with chloroform and then dipping into a chloroform solution of PVK and withdrawing slowly; D, evaporation of chloroform and shrinkage of liquid film; E, blowing with humid N_2 slowly; F, dipping into dilute chloroform solution and withdrawing immediately; G, complete evaporation of chloroform and water.

Preparation of Self-Assembled Monolayers (SAMs) Patterned Gold Substrate. The overall procedure for fabricating ordered bull's-eye-like structures on patterned SAMs is depicted in the Scheme 1. The microcontact printing (μCP) method for alkanethiols on gold was followed as described by Kumar et al.[43] Photoresist was spin-coated on the cleaned glass slide (with spinning speed 3000 rpm for 1 min and the resulting resist film thickness being 2 μm) and patterned using conventional photolithography techniques. Then the μCP stamp was fabricated by casting PDMS on the photolithographically prepared glass master. In all experiments, μCP was carried out with an elastomeric stamp on whose surface there was an ordered array of raised circles that were 12 μm in diameter and separated by 5 μm. A 2 mM solution of MHA in ethanol was used to ink the stamp. After evaporation of the solvent, the PDMS stamp was dried under N_2 for several minutes and brought in contact with the gold substrate for 5−10 s. And then the substrate was immersed into a 2 mM solution of HDT for 5 min to form a SAM on the bare gold regions. The sample was finally rinsed with absolute ethanol to remove the excess alkanethiol and dried with N_2.

Preparation of 2D Ordered Dot Arrays. The SAM-patterned gold substrate was dipped into the chloroform solution of PVK and withdrawn at a constant velocity of 0.5 cm s^{-1}. The concentration of chloroform solution ranged from 20 to 60 mg mL^{-1}. After chloroform completely evaporated at room temperature, the 2D ordered PVK dot arrays were left on the surface of the gold substrate. Other materials were also introduced into this experiment to expand the application. For example, the chloroform solution of DCJTB, CPEY, and PS were used to repeat the experiment, whose concentrations were 30, 30, and 50 mg mL^{-1} respectively.

Preparation of Bull's-Eye-Like Structure Arrays. An N_2 flow saturated with water vapor was streamed across the surface with the ordered PVK dot arrays pattern through a glass nozzle

(37) Pan, Z.; Donthu, S.; Wu, N.; Li, S.; Dravid, V. *Small* **2006**, *2*, 274.
(38) Jacobs, H. O.; Tao, A. R.; Schwartz, A.; Gracias, D. H.; Whitesides, G. M. *Science* **2002**, *296*, 323.
(39) Divliansky, I.; Mayer, T. S.; Holliday, K. S.; Crespi, V. H. *Appl. Phys. Lett.* **2003**, *82*, 1667.
(40) Jeon, S.; Menard, E.; Park, J. U.; Maria, J.; Meitl, M.; Zaumseil, J.; Rogers, J. A. *Adv. Mater.* **2004**, *16*, 1369.
(41) Smay, J. E.; Cesarano, J.; Lewis, J. A. *Langmuir* **2002**, *18*, 5429.
(42) Lee, J.; Isobe, T.; Senna, N. *J. Colloid Interface Sci.* **1996**, *177*, 490.
(43) Kumar, A.; Biebuyck, H. A.; Whitesides, G. M. *Langmuir* **1994**, *10*, 1498.

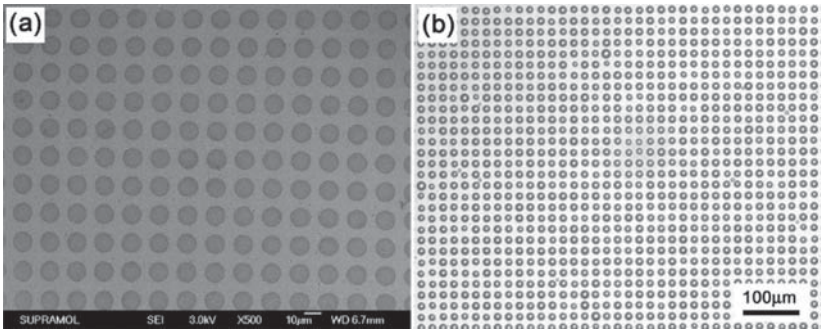

Figure 1. (a) Scanning electron microscope (SEM) image of patterned SAMs on a gold surface. The diameter of the circle is about 12 μm and the distance between two neighboring circles is about 5 μm. (b) Optical micrograph of ordered arrays of condensed water droplets formed on the SAMs-pattern surface. The water droplets coincide well with the hydrophilic regions shown in part a.

immediately. The condensate water droplets covered the hydrophilic circles on substrate for protecting PVK dot arrays. The inspection of water condensation on the patterned gold substrate was carried out in situ using an optical microscope. Then, the water-droplets-covered substrate was dipped into another dilute chloroform solution and withdrawn immediately. With the complete evaporation of chloroform and water, ordered bull's-eye-like structure arrays were obtained. Various kinds of materials were used to fabricate ring arrays, such as PVK, DTQA and Fe_3O_4 nanoparticles, whose concentrations are 0.5, 0.5, and 0.4 mg mL^{-1}, respectively.

Characterization. Scanning electron microscopy (SEM) images were made on a JEOL JSM6700F field emission scanning electron microscope with primary electron energy of 3 kV. Atomic force microscopy (AFM) image was measured with Digital Instruments NanoScope IIIa in tapping mode. Magnetic force microscopy (MFM) images were measured with Digital Instruments NanoScope IIIa by a multimode using single-crystal silicon cantilevers with pyramidal tips coated with a Co−Cr alloy. The optical and fluorescent images were recorded on an Olympus BX51 microscope (in reflection mode) and were captured with a MVC1000 USB2.0 megapixel camera. A HR4000 UV−visible spectrometer (from Ocean Optics) was used to measure the fluorescence spectrum.

Results and Discussion

Formation of 2D Ordered Dot Arrays on SAMs-Patterned Surface. Figure 1a shows the scanning electron microscope (SEM) image of SAMs-patterned surface on gold substrate. As the previous work in literature has reported, SEM is able to form images of patterns of SAMs of alkanethiolates adsorbed on gold, and the SEM image provided material contrast on the gold surface, where the darker regions represented the hydrophilic COOH-SAM and the brighter regions represented the CH_3−SAM respectively.[44] Therefore, from Figure 1a, we could clearly observe the SAMs pattern was replicated from the PDMS stamp completely, in which, the average diameter of the hydrophilic circle was approximately 12 μm and the distance between two neighboring circles was approximately 5 μm just like the PDMS stamp. Figure 1b is an optical micrograph of the regular arrays of condensed water droplets formed on the SAMs-patterned gold substrate, which shows that the pattern was highly ordered in a large area with few defects. The image represents the level of perfection, order, scale, and area that could be routinely achieved using our method. We could even obtain an ordered area of several square centimeters in our experiments. The patterned condensation image also reflected the difference between the dispersed hydrophilic circles and the continuous hydrophobic region, which coincided well with the material contrast shown in the SEM image of Figure 1a.

After being washed with chloroform, the SAMs-patterned gold substrate was dipped into a 30 mg mL^{-1} chloroform solution of PVK and withdrawn at a constant velocity of 0.5 cm s^{-1}. When chloroform evaporated completely, 2D ordered PVK dot arrays on SAMs patterned gold substrate were obtained. Figure 2a is the fluorescent image of a large area of 2D ordered PVK dot arrays, which exhibit intensive blue luminescence by the excitation of an ultraviolet (UV) emission source. Figure 2b shows the SEM image of ordered PVK dot arrays on SAMs-patterned gold substrate, and the high-magnification SEM image shows that the dots were formed in the middle of circles accurately. Here, period of dot arrays were consistent with period of patterned SAMs. Therefore, arrangement of dot arrays could be simply adjusted by changing different PDMS stamps. Figure 2c gives an atomic force microscope (AFM) (in tapping mode) image, and the corresponding cross sectional analysis image of Figure 2c shows that the dots are on average 2.1 μm in diameter and 112 nm in height. As we have concluded, the dewetting behavior was strongly influenced by the thickness of the liquid film which was controlled by the concentration of polymer solution on flat surface.[45] In present experiments, it was found that the final dimension and morphology of ordered dot arrays were also dependent on the concentration of PVK solution. Through a large number of experiments, the 2D ordered PVK dot arrays could be obtained in the range of the concentrations of PVK solution from 20 to 60 mg mL^{-1}; while, we could not obtain the ordered PVK dot arrays in the condition that the concentrations were less than 20 mg mL^{-1} or higher than 60 mg mL^{-1} by dip-coating. The reason could be that deposition and dewetting of thin liquid film were related to the concentration of solution, which would be investigated later. Figure 2d shows the relationship curve between the concentration of PVK solution and the average heights of dot arrays which were produced from the same experimental conditions. The average diameter of the dot arrays in these samples was in the range of 1.5 and 2.2 μm. By adjusting the concentration of the solution from 20 to 60 mg mL^{-1}, the average height of the dots changed from 82 to 257 nm, as shown in Figure 2d. The diameter of the dot increased as the concentration increased, which made it possible to control the dimension of the dot by simply changing the solution concentration.

Mechanism of the Formation of Ordered Dot Arrays. Figure 3 is the schematic drawing of the dot arrays formation process on the SAMs-patterned surface. During dip coating, a

(44) López, G. P.; Biebuyck, H. A.; Whitesides, G. M. *Langmuir* **1993**, *9*, 1513.

(45) Darhuber, A. A.; Troian, S. M.; Davis, J. M.; Scott, M. M.; Wagner, S. *J. Appl. Phys.* **2000**, *88*, 5119.

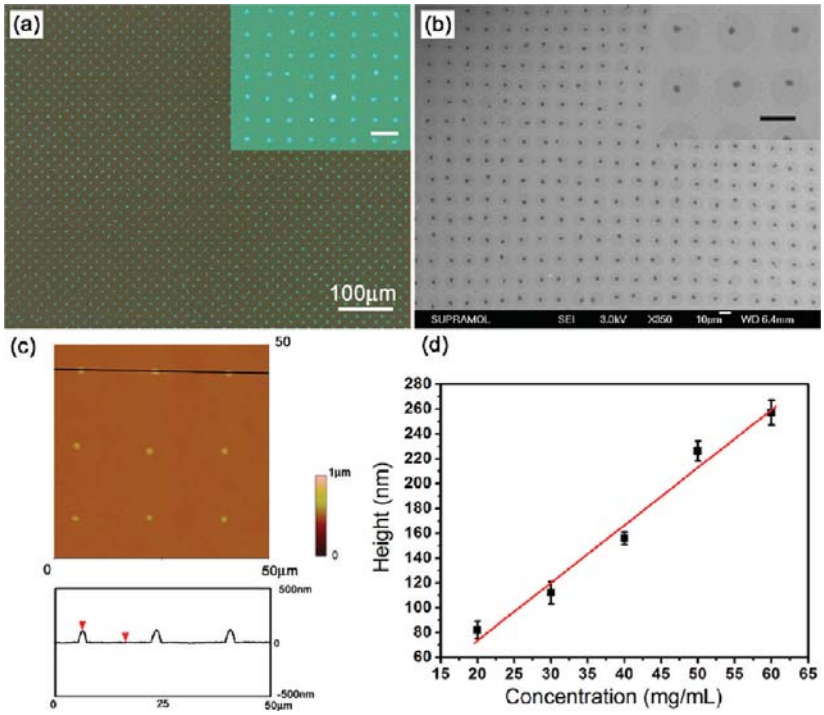

Figure 2. (a) Large-area fluorescent image of 2D ordered PVK dot arrays on gold substrate with patterned SAMs. The inset shows a magnified image; the scale bar is 20 μm. (b) SEM image of 2D ordered PVK dot arrays. The inset shows a magnified image; the scale bar is 10 μm. (c) Atomic force microscope (AFM) (in tapping mode) image of 2D ordered PVK dot arrays, contained height image and section analysis; (d) Relationship curve between the concentration of PVK solution and the average height of dots.

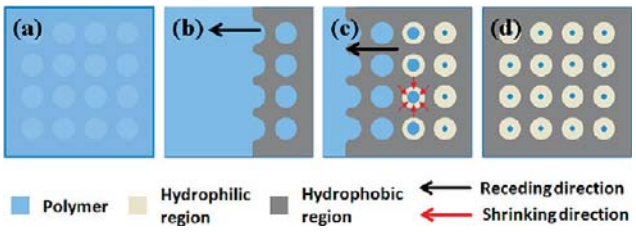

Figure 3. Schematic drawing of the dot arrays formation process on the SAMs-patterned surface. Key: (a) thin film on the SAMs-patterned surface; (b) SAMs-direct dewetting with evaporation of chloroform; (c) shrinkage of disk-like liquid films under surface tension; (d) ordered polymer dot arrays on SAMs-patterned gold substrate.

liquid film of chloroform solution was initially deposited on the SAMs-patterned surface. And then the liquid film became unstable as it was thinned by the evaporation of chloroform (Figure 3a). When the liquid film was thinned below a critical thickness by further evaporation of chloroform, dewetting took place due to spinodal decomposition or heterogeneous nucleation[46,47] (initiated by some intrinsic or extrinsic defects in the liquid film or on the surface of the SAMs). Thermodynamically, the stability of a fluid film is assumed to be governed by the change in Gibbs-free-energy[48] and a thermodynamic system will spontaneously tend to go to the lowest Gibbs-free-energy state. Accordingly, the liquid film selectively covered the circular hydrophilic regions which were in the higher Gibbs-free-energy state; the purpose was to lower the system energy (Figure 3b). It was worth pointing out that the disk-like liquid films on the hydrophilic circles were not in the lowest Gibbs-free-energy state; namely, it was only an intermediate state. Because the disk-like structure was not stable under the role of surface tension of chloroform solution, the disk-like liquid film would tend to shrink into a droplet to lower the energy of the system (Figure 3c). Finally, with the complete evaporation of chloroform, the ordered polymeric dot arrays were fabricated on the SAMs-patterned surface (Figure 3d). The corresponding optical micrographs were shown in the Supporting Information Figure 1.

The surface tension played an important role in the shrinkage process of the disk-like liquid film. As we known, surface tension of solution was related to intermolecular force: the stronger the intermolecular forces were, the greater the surface tension would be.[49] According to the principle of "similar dissolves", in the chloroform solution of polymer, the intermolecular forces between solvent and solute were stronger; correspondingly, the surface tension was stronger, which would result in shrinkage of the thin disk-like films on the hydrophilic regions as a result of the minimization of surface free energy, such as PVK and PS, as shown in Figure 2a and Figure 4a. On the contrary, in chloroform solution of the small molecular-based organic complex, the intermolecular forces between complex and chloroform were rather weak, which leading to the surface tension of these solutions was weaker than the chloroform solution of polymer. When the chloroform evaporated completely, the shrinkage of the disk-like liquid films of the complex solution was not sufficient under the weaker surface tension. As a result, the ordered disk-like structure arrays were formed on the SAMs-patterned gold substrate, such as CPEY and DCJTB, as shown in Figure 4, parts b and c. Accordingly, the formation of ordered dot arrays resulted from two key factors which were the process of SAMs-directed

(46) Herminghaus, S.; Jacobs, K.; Mecke, K.; Bischof, J.; Fery, A.; Ibn-Elhaj, M.; Schlagowski, S. *Science* **1998**, *282*, 916.
(47) Mitlin, V. S. *J. Colloid Interface Sci.* **1993**, *156*, 491.
(48) Schäer, E.; Thurn-Albrecht, T.; Russell, T. P.; Steiner, U. *Nature* **2000**, *403*, 874.
(49) Scholberg, H. M.; Guenthner, R. A. *J. Phys. Chem.* **1953**, *57*, 923.

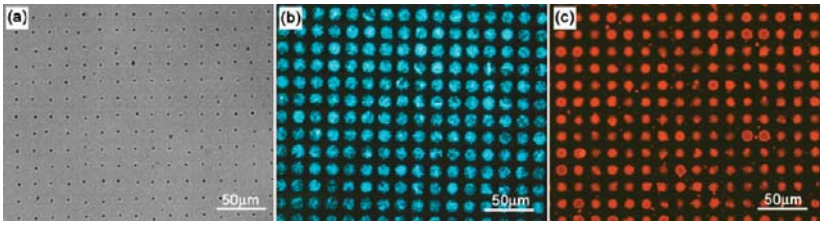

Figure 4. (a) Optical image of 2D ordered PS (the molecular weight is 3600) dot arrays on SAMs patterned gold substrate. Fluorescent image of 2D ordered CPEY (b) and DCJTB (c) disk arrays on SAMs patterned gold substrate.

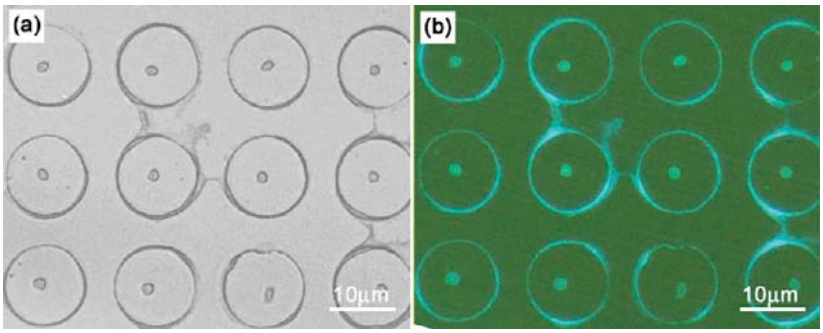

Figure 5. Optical image (a) and fluorescent image (b) of ordered PVK/PVK bull's-eye-like structure arrays on gold substrate.

dewetting and the role of surface tension. After analysis and comparison, the PVK had been chosen for further experiments due to fine controllability and functional.

Fabrication of Ordered PVK Bull's-Eye-Like Structure Arrays. As the experiments above, the 2D ordered PVK dot arrays were fabricated on the SAMs-patterned surface successfully. When we blew water vapor onto this surface slowly, the vapor would tend to condense at the original hydrophilic regions. We could observe the process that the small water droplets were covering or discovering the PVK dots gradually in situ by optical microscope, as shown in Supporting Information Figure 2. By controlling period and speed of the blowing, the PVK dot arrays on the substrate were covered by the individual water droplets completely. It is proved that the chemical properties of the SAMs on the gold substrate were reserved. In order to form the 2D ordered ring arrays, the concentration of solution should be below the critical concentration. Therefore, we put the substrate with ordered dot arrays under water droplets into 0.5 mg mL^{-1} PVK chloroform solution, and withdrawn immediately. With the complete evaporation of solvent and water, 2D ordered PVK ring arrays were obtained on the patterned surface of gold substrate by the water-droplets-directed and concentration-controlled dewetting process. Meanwhile, the dot arrays that protected by water droplets were exposed to us now. Namely, the ordered PVK (dot)/PVK (ring) bull's-eye-like structure arrays were fabricated successfully. In this process, the ordered water droplets on the hydrophilic regions could subsequently serve as shields, resulting in that the PVK dots were not dissolved by chloroform. Figure 5a and b are optical and fluorescent images of the homogeneous PVK bull's-eye-like structure arrays on gold substrate, respectively. We could observe that both dots and rings in the ordered arrays exhibited intensive blue luminescence by the excitation of an UV emission source (Figure 5b). From the image (Figure 5a), we could also observe that the dots in the middle of the bull's-eye-like structures maintained the original morphology, and there was no residues left between dot and ring, which proved that the protecting of water droplets was successful. However, a small amount of residue was found between the adjacent rings, likely because that the dewetting behavior was incomplete in the continuous hydrophobic region. As we had mentioned in previous work, if the solution concentration was reduced further, these defects could be avoided.[27] Shortly, since the fabrications of the dot arrays and ring arrays were separated by the water droplets completely, a variety of materials could be introduced to this system. Accordingly, the fabrication of ordered heterogeneous bull's-eye-like structures arrays would be feasible by using this two-step method.

Fabrication of Ordered Heterogeneous Bull's-Eye-Like Structure Arrays. We have proposed that it is possible to create the ring arrays as long as the simple conditions are satisfied, which could be extended to various materials. The only requirement seems to be that these materials should be dissolved or dispersed in a water-immiscible and volatile organic solvent. In this part, light-emitting small molecular-based organic complex DTQA and oil-soluble Fe_3O_4 magnetic nanoparticles were used to fabricate the heterogeneous bull's-eye-like structure arrays. The details of ring arrays formation have been systematic studied, in which, the dimension of ring arrays could be controlled accurately. Therefore, ordered DTQA ring arrays could be obtained simply by the concentration-controllable dewetting behavior, as shown in Supporting Information Figure 3.

The patterned substrate with PVK dot arrays was formed by dip coating from 60 mg mL^{-1} chloroform solution of PVK according to previous operating steps, and blew with humid N_2 slowly. At the same time, we could control the saturation of water droplets on the surface of hydrophilic regions, through in situ optical microscope observation. When the water droplets were in a steady state, we put the substrate with water droplets arrays into the 0.5 mg mL^{-1} DTQA chloroform solution, and withdrawn immediately. With the complete evaporation of water and chloroform, ordered heterogeneous fluorescent bull's-eye-like structure arrays have been fabricated successfully. Parts a and b of Figure 6 are optical and fluorescent images of the ordered heterogeneous PVK/DTQA bull's-eye-like structure arrays, respectively. We could observe that the morphology of the bull's-eye-like structures is quite uniform in the inset of Figure 6a. From the fluorescent image Figure 6b, we could clearly see that the dots pattern in the center exhibit intensive blue luminescence and the

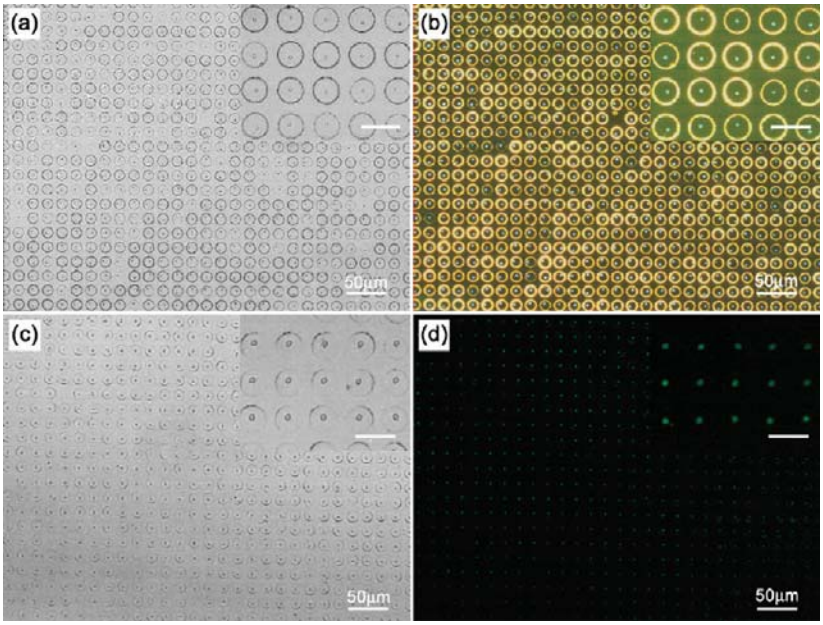

Figure 6. Optical image (a) and fluorescent image (b) of ordered PVK/DTQA bull's-eye-like structure arrays on gold substrate from the same sample. The inset shows a magnified image; the scale bar is 20 μm. Optical image (c) and fluorescent image (d) of ordered PVK/Fe_3O_4 nanoparticles bull's-eye-like structure arrays on gold substrate from the same sample. The inset shows a magnified image; the scale bar is 20 μm.

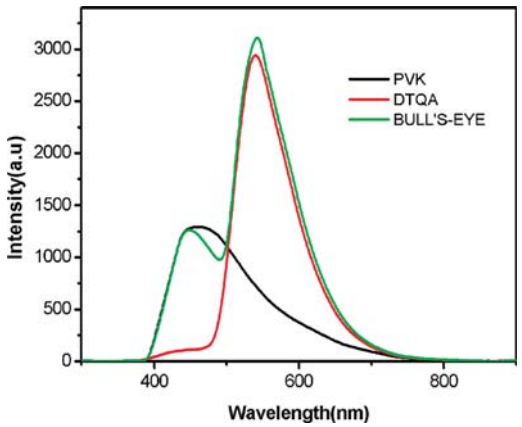

Figure 7. Photoluminescence (PL) spectra of PVK dot arrays, DTQA ring arrays and PVK/DTQA bull's-eye-like structure arrays.

rings pattern exhibit intensive yellow-green luminescence under UV excitation. Through comparative analysis of the images of PVK dot arrays (Figure 2a), DTQA ring arrays (Supporting Information Figure 3) and PVK/DTQA bull's-eye-like structure arrays (Figure 6b), we considered that the formation of heterogeneous bull's-eye-like structure arrays did not affect their respective luminescent properties by this strategy. Figure 7 is photoluminescence (PL) spectra of PVK dot arrays, DTQA ring arrays and PVK/DTQA bull's-eye-like structure arrays. Here, PVK showed blue PL with a peak at around 458 nm. DTQA showed green PL with a peak at around 542 nm. The fluorescent PVK/DTQA bull's-eye-like structure arrays yield a distinct multipeak spectrum, correlating well with the composition of two fluorescent materials, and the peaks match the original PL spectra well with negligible shifts.

Not only fluorescent materials but also magnetic nanoparticles could be used to fabricate ring arrays. The oleic-acid-modified magnetite nanoparticles we used were synthesized according to literature.[42] The dispersibility and stability of magnetite in chloroform were improved by the polymer coating.[50] Coating with a thin layer of polymer on the magnetite nanoparticles could make the property of the particles similar to polymer, increase the nonpolarity of the particles, and promote the stability of magnetite nanoparticles in chloroform. As a result, the oleic acid modified magnetite nanoparticles were used to develop the ordered ring arrays.[51] Magnetic nanoparticles chloroform solution with concentration of 0.4 mg mL^{-1} was used to repeat the experiment above to fabricate the fluorescent/magnetic multifunctional heterogeneous bull's-eye-like structure arrays. Figure 6c shows that optical image of ordered PVK/Fe_3O_4 nanoparticles bull's-eye-like structure arrays, and we could clearly observe each regular bull's-eye-like structure composed of a dot and a ring in the photograph. While, from the fluorescent image of Figure 6d, we could only observe the PVK dot arrays with blue fluorescence, and could not observe the Fe_3O_4 ring arrays on the substrate under UV excitation, which is because that the Fe_3O_4 nanoparticles could not be excited by the UV emission source.

In order to verify the magnetism of the magnetite rings, PVK/Fe_3O_4 bull's-eye-like structure arrays on gold substrate were further investigated by magnetic force microscopy (MFM), shown in Figure 8. MFM is a powerful tool to study the magnetic properties of patterned structures. Before imaging, the tip, coated with a ferromagnetic thin film, was magnetized with an external magnetic field. The magnetic force was then detected by measuring the phase shift in the cantilever oscillation, a consequence of the magnetic interactions acting on the tip. Figure 8a shows the height mode MFM image and corresponding cross sectional analysis image of a sample fabricated from a 0.4 mg mL^{-1} chloroform solution of the Fe_3O_4 nanoparticles. As shown in Figure 8a, the dots are approximately 1.8 μm in width, 250−265 nm in height; and the rings approximately 1.6 μm in width, 560−640 nm

(50) An, L.; Li, W.; Nie, Y.; Xie, B.; Li, Z.; Zhang, J.; Yang, B. *J. Colloid Interface Sci.* **2005**, *288*, 503.
(51) Matsuno, R.; Yamamoto, K.; Otsuka, H.; Takahara, A. *Chem. Mater.* **2003**, *15*, 3.

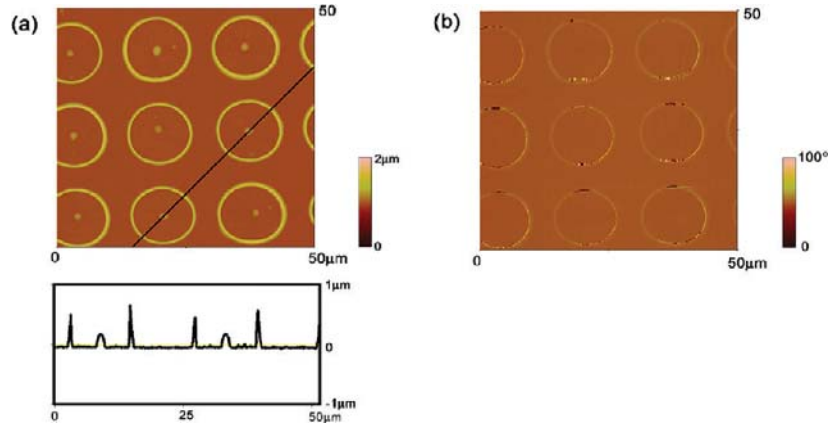

Figure 8. (a) Height mode image of magnetic force microscopy (MFM) and corresponding cross sectional analysis image of ordered PVK/Fe_3O_4 nanoparticles bull's-eye-like structure arrays. (b) Corresponding phase shift mode MFM image of PVK/Fe_3O_4 nanoparticles bull's-eye-like structure arrays in part a.

in height, and 12 μm in diameter. Figure 8b is the corresponding phase shift mode MFM image of Figure 8a. The comparison of these two pictures shows that the pattern imaged in the height mode coincided well with the one imaged in the phase shift mode. The bright signals in the corresponding phase shift mode MFM image indicated the presence of magnetic substance in the rings; namely, the highly ordered Fe_3O_4 ring arrays were really magnetic. From Figure 8b, the signals of dot arrays could not be detected, which proved that the dots were made up of PVK without magnetic.

Conclusion

In summary, we have demonstrated a versatile method to fabricate ordered homogeneous and heterogeneous bull's-eye-like arrays on the SAMs-patterned surface of a gold substrate through a simple approach. First, we fabricated the PVK dot rings on the SAMs-patterned gold substrate by SAMs-directed dewetting; at the same time, we optimized conditions of the dot formation of different materials. Second, as the reservation of chemical properties on SAMs, we obtained the ordered ring arrays on the dot arrays patterned surface under the protecting of water droplets by water-droplets-directed and concentration-controlled dewetting process. Finally, the ordered bull's-eye-like structure arrays had been fabricated on the gold substrate. Since both experimental steps were relatively independent, the bull's-eye-like structure that we fabricated could be not only homogeneous but also heterogeneous. We had fabricated the bull's-eye-like structure arrays of PVK/PVK, PVK/DTQA, and PVK/Fe_3O_4 nanoparticles separately, and characterized the properties of fluorescence and magnetism. Accordingly, diverse material could be introduced to the current system, such as fluorescent materials, electroconductive materials and magnetic materials as long as the simple conditions are satisfied. These heterogeneous bull's-eye-like structure arrays may have potential applications including photoelectric devices, catalytic surfaces, field emission devices and integrated magnetic, gas, and biochemical sensors.

Acknowledgment. This work was supported by the National Natural Science Foundation of China (Grant Nos. 20534040, 20874039, 50703015) and the National Basic Research Program of China (2007CB936402).

Supporting Information Available: Figures showing the schematics of the molecular structure of CPEY, DCJTB, and DTQA, the corresponding optical micrographs verified the presentations of the mechanisms of dot arrays formation, serial optical images of process of water droplet evaporation on the dot arrays pattern and the fluorescent image of ordered DTQA ring arrays. This material is available free of charge via the Internet at http://pubs.acs.org.